Exfoliation of alpha-germanium: a covalent diamond-like structure

Carlos Gibaja,[1] David Rodríguez-San-Miguel,[1] Wendel S. Paz,[2,3] Iñigo Torres,[1] Elena Salagre,[2] Pilar Segovia,[2] Enrique G. Michel,[2] Mhamed Assebban,[4,5] Pablo Ares,[2,6] David Hernández-Maldonado,[7,8] Quentin Ramasse,[8,9] Gonzalo Abellán,[4,5] Julio Gómez-Herrero,[2,10] Maria Varela,[7] Juan José Palacios,[2,10] Félix Zamora[1,]*

Dr. Carlos Gibaja, Dr. David Rodríguez-San-Miguel, Iñigo Torres, Dr. Félix Zamora.
Departamento de Química Inorgánica, Institute for Advanced Research in Chemical Sciences (IAdChem) and Condensed Matter Physics Center (IFIMAC), Universidad Autónoma de Madrid, 28049, Madrid, Spain.
E-mail: felix.zamora@uam.es

Dr. Wendel S. Paz.
Departamento de Física, Universidade Federal do Espírito Santo, Vitória, ES 29075-910, Brazil.
E-mail: wpascal1@gmail.com

Elena Salagre, Dr. Pilar Segovia, Dr. Enrique G. Michel, Dr. Pablo Ares, Prof. Julio Gómez-Herrero, Dr. Juan José Palacios.
Departamento de Física de la Materia Condensada and Condensed Matter Physics Center (IFIMAC). Universidad Autónoma de Madrid, 28049, Madrid, Spain.
E-mail: julio.gomez@uam.es

Dr. Mhamed Assebban, Dr. Gonzalo Abellán.
Instituto de Ciencia Molecular (ICMol). Universidad de Valencia, Catedrático José Beltrán 2, 46980, Paterna, Valencia, Spain.
E-mail: gonzalo.abellan@uv.es

Dr. Mhamed Assebban, Dr. Gonzalo Abellán.
Department of Chemistry and Pharmacy & Joint Institute of Advanced Materials and Processes (ZMP). Friedrich-Alexander-Universität Erlangen-Nürnberg (FAU), Dr.-Mack-Straße 81, 90762, Fürth, Germany.
E-mail: gonzalo.abellan@uv.es

Dr. Pablo Ares.
Department of Physics and Astronomy and National Graphene Institute, University of Manchester, Oxford Road, Manchester M13 9PL, UK.
E-mail: pableras.ares@gmail.com

Dr. David Hernández-Maldonado, Dr. Maria Varela
Facultad de CC. Físicas & Instituto Pluridisciplinar. Universidad Complutense de Madrid. 28040, Madrid, Spain.
E-mail: mvarela@fis.ucm.es

Dr. David Hernández-Maldonado, Dr. Quentin Ramasse
SuperSTEM. SciTech Daresbury Science and Innovation Campus. Block J. Keckwick Lane, Daresbury, WA4 4AD, UK.
E-mail: q.m.ramasse@leeds.ac.uk

Dr. Quentin Ramasse
School of Chemical and Process Engineering & School of Physics and Astronomy, University of Leeds, Leeds LS2 9JT, UK.
E-mail: q.m.ramasse@leeds.ac.uk

Prof. Julio Gómez-Herrero, Dr. Juan José Palacios
Instituto Nicolás Cabrera (INC), Universidad Autónoma de Madrid, 28049, Madrid, Spain.
E-mail: julio.gomez@uam.es

Abstract

Two-dimensional (2D) materials opened a new field in materials science with outstanding scientific and technological impact. A largely explored route for the preparation of 2D materials is the exfoliation of layered crystals with weak forces between their layers. However, its application to covalent crystals remains elusive. Herein, one step further has been gone by introducing the exfoliation of germanium, a narrow band gap semiconductor presenting a 3D diamond-like structure with strong covalent bonds. In this work, pure α-germanium is exfoliated following a simple one-step procedure assisted by wet ball-milling, allowing gram-scale fabrication of high-quality layers with large lateral dimensions and nanometer thicknesses. The generated flakes are thoroughly characterized by different techniques, giving evidence that the new 2D material exhibits band gaps that depend on both the crystallographic direction and the number of layers. Besides potential technological applications, our work is also of interest for the search of 2D materials with new properties.

Since the initial isolation and characterization of the first one-atom thick material, graphene, the search for new two-dimensional (2D) materials has attracted great attention due to their fundamental outstanding physical and chemical properties as well as their potential technological impact.[1] Apart from synthesis methods based on bottom-up approaches, *e.g.* chemical vapour deposition, these 2D nanostructures have been largely prepared using top-down techniques,[2] such as micromechanical or liquid phase exfoliation (LPE), in which the typical starting materials are van der Waals (vdW) layered crystals. This has allowed not only to study the physical properties of pristine nanolayers isolated on different surfaces and the fabrication of novel proof-of-concept devices, but also to generate stable suspensions containing single/few-layers with a variety of properties and applications. Here, we can highlight heterogeneous catalysis, fabrication of filtration membranes, novel electrodes for supercapacitors, or inks for flexible electronics, to name a few.[3] Importantly, an initial layered crystal structure with weak interlayer interactions was commonly accepted as a pre-requisite for the starting materials to be exfoliated, restricting the source to the known laminar crystals. Very recently, the exfoliation of a three-dimensional (3D) crystal of iron oxide has been reported in a seminal work,[4] opening a window of opportunities for new materials. This result suggests that exfoliation is not limited to layered vdW solids, highlighting the importance of other parameters such as the energy of cleavage planes or the stabilization energy of the nanolayers that facilitate exfoliation in a more general class of 3D materials. Unfortunately, iron oxide is an ionic compound with limited technological applications. For instance, electronics technology is nowadays dominated by semiconductors with strong covalent bonds, as for instance, silicon or germanium. In the latter case, it is remarkable that, besides optoelectronic applications of germanium in bulk, *e.g.* optical fibres or infrared detectors, this semiconductor, with a band gap *ca.* 0.67 eV, is also considered a promising candidate for the fabrication of high-performance batteries.[5] However, research in these fields has been limited so far by the lack of germanium nanostructures, which are essentially reduced to a few examples

of nanoparticles, in addition to novel germanium forms such as germanane (GeH),[6] a single-layer crystal of germanium bonded to hydrogen similar to graphane, and germanene,[7] a structural analog to graphene that has only been prepared under stringent ultra-high vacuum (UHV) conditions. Therefore, the preparation of novel nanostructures of germanium in the form of nanolayers is of high scientific and technological interest and is the objective central topic of this work.

Herein we demonstrate that the wet ball-milling technique can be successfully used with bulk α-germanium crystals to produce α-germanium nanolayers (α-Ge NLs) in a process that can be easily up-scaled to gram production. This procedure only requires a mixture of isopropanol (ⁱPrOH)-water. Importantly, it does not need the addition of further surfactants that, in many cases, results in products difficult to manipulate. Besides, the α-Ge NLs can be easily redispersed using a shear-mixer, yielding very stable suspensions, over weeks, of micron-scale nanolayers even in ambient conditions. As we shall see, the so-formed α-Ge NLs show the absence of side-products, no significant oxidation, and high-crystallinity. Remarkably, theoretical calculations predict a thickness-dependent band gap of these nanolayers that is confirmed further by electron energy-loss spectroscopy (EELS) of α-Ge NLs with different orientations. This work, summarized graphically in **Figure 1**, evidences the possibility of creating a very general class of new 2D structures using LPE and covalent crystals as precursors.

We carried out LPE of α-germanium crystals (Figure 1) using a wet ball-milling route for 60 min at 3000 rpm, of a combination of ground α-germanium crystals with a small volume of a 4:1 ⁱPrOH-water mixture. We dried the so-formed mixture under vacuum yielding a homogeneous powder of the above introduced α-Ge NLs. We have successfully tested the scalability of this procedure up to 1 gram for a single batch of reaction (Experimental Section). The obtained material can be dispersed using a shear-mixer device in a mixture of 4:1 ⁱPrOH-water for 60 min at 25000 rpm. We then centrifuged the resulting suspension for 3 min at 3000

rpm in order to get rid of the non-exfoliated material and to produce a homogeneous and stable dispersion showing Faraday-Tyndall effect (Figure 1), with an initial concentration of *ca.* 0.87 g·L^{-1} as determined by flame atomic absorption spectrometry (Experimental Section). Interestingly, after one week of sedimentation, suspensions undergo a concentration decrease of only *ca.* 30 %, indicating good stability. Moreover, we have observed that after long periods of sedimentation, the suspensions recover their initial concentration values by re-suspending them using the shear-mixer device for 5 min.

Remarkably, the selection of the right solvent solution is not trivial. Previous experiments carried out to exfoliate bulk α-germanium crystals under similar experimental conditions but using other solvents or mixtures of solvents gave rise either to GeO$_2$ (JCPDS card No. 43-1016) or mixtures of α-Ge and GeO$_2$ species (Supporting Information 5).

Figure 2a shows scanning electron microscopy (SEM) images of bulk α-germanium crystals and Figure 2b α-Ge NLs obtained after the wet ball-milling process (for additional images, see Figure S1 and S2). This technique allows us an initial confirmation of the 2D morphology of the obtained α-Ge NLs upon re-dispersing and centrifuging the powder in ^{i}PrOH-water. Drop-casting deposition from the α-Ge NLs suspension allows the isolation of α-Ge NLs (Figure 2c). Additionally, we corroborated the 2D morphology by optical and atomic force microscopy (AFM). Figure 2d portrays an optical microscopy image where a collection of flakes isolated on a SiO$_2$ substrate is observed. The thickness of the flakes correlates with the colour, corresponding dark blue to thicknesses in the 10 nm range, serving as a guide for subsequent AFM characterization. Figure 2e shows a characteristic topographic image obtained by AFM of one of these α-Ge NLs isolated on a SiO$_2$ substrate (Figure 2d). Figure 2g shows the height profile along the blue line in Figure 2e, displaying terraces with well-marked steps (Figure S4). It has to be taken into account that apparent AFM heights of layers obtained by LPE techniques can be overestimated due to residual solvent[8] as well as contributions from effects such as

5

capillary and adhesion forces.[9] We also obtained fine structural details of the α-Ge NLs analysing high-resolution AFM topographic images. Interestingly, Figure 2f reveals the expected hexagonal symmetry for the α-germanium (111) plane, pointing to an excellent crystal quality. A statistical analysis of α-Ge NLs isolated on SiO_2 substrates further confirms their bidimensional character, with heights between 5 and 40 nm and typical lateral sizes of a few microns (Figure 2h and S5).

We also confirmed the crystallinity and phase purity of the α-Ge NLs by powder X-ray diffraction (PXRD). **Figure 3a** shows a comparison between the PXRD patterns of the bulk α-germanium crystals and the α-Ge NLs, showing that after the exfoliation process, the nanolayers do not suffer any measurable change on their crystalline structure compared to that expected for the canonical α-phase of germanium (JCPDS card No. 03-065-0333). There is a clear change on peaks relative intensity on passing from bulk to NL, which is indicative of passing from an isotropic crystal to preferential orientations typical of layered material. In this case, the relative intensity of the (111) and (311) peaks increases. This agrees with the fact that the preferential orientations seem to be along with the (111) and (311) directions.

PXRD does not provide information on the chemical state of the NL surface. In order to gain insight on this issue, we carried out X-ray photoelectron spectroscopy (XPS) using synchrotron light of 650 eV and Mg K_α radiation (1253.6 eV, see also Supporting Information section 8) on α-Ge NLs deposited on HOPG. We measured the Ge 3p core level with a binding energy of 122 eV (Figure 3b and S12). The surface sensitivity is different for each photon energy, as the electron mean free path changes from ~1.1 nm (for hν = 650 eV) to ~1.9 nm (for hν = 1253.6 eV). The Ge 3p core level is deconvoluted in three components 1, 2, and 3 (Figure 3b and Figure S12). Component 1 is assigned to elemental germanium (unoxidized). Component 2 (shift of 2.5 eV wrt Ge) corresponds to Ge^{3+}, but it may include a contribution from Ge^{2+}.[10] Component 3, with a shift of 4.0 eV wrt to Ge, matches Ge^{4+}, i.e. GeO_2.[10] The ratio Ge/GeO_2 changes

6

dramatically when the escape depth increases, revealing that the GeO_2 corresponds to a surface layer of ~1 nm thickness. This value is compatible with the expected thickness for a layer of native oxide on the Ge flakes due to air exposure before the XPS measurements.[10]

Additional information can be obtained from Raman spectroscopy of exfoliated α-Ge NLs. Figure 3c portrays a Raman spectrum with the typical out-of-plane Raman mode (E_2) of crystalline α-phase germanium.[3],[6] The observed sharp peak, which is centered at 300 cm^{-1}, is shifted towards higher wavenumbers by 3 cm^{-1} compared to bulk crystalline germanium (E_2 peak at 297 cm^{-1}).[8],[11] Such a blue shift has also been previously observed in the case of some Ge nanoparticles, [8],[12] thus confirming, the successful formation of Ge nanostructures with a high degree of crystallinity. Furthermore, Figure 3d shows a mapping of the characteristic E_2 Raman mode over the area marked with the dashed rectangle in the optical microscopy image in Figure S11a. A combination between Figure 3d and the AFM topographic scan over the same region allowed the unambiguous identification of α-Ge NLs (Figure S11c). As the Raman set up was tuned for high surface sensitivity, the observed oxygen presence in the XPS data is restricted to the passivation of the dangling bonds always present on the surface or at most to the native oxide grown during air exposure. We have to notice that the surface sensitivity of Raman is probably much lower (unless we had used SERS, which was not the case)than in XPS. This is why Raman cannot detect the passivation oxide layer of Ge-NLs.

In turn, the XPS mean free path used in Figure S12 (bottom spectrum) is *ca*. 1 nm. As we see a small unoxidized Ge peak, we estimate that the oxide thickness is *ca*. 1 nm or less. This agrees with the fact that the native oxide thickness for Ge is *ca*. 1 nm,[10] and that it needs *ca*. 1 week of air exposure to grow. The analysed flakes were exposed to air several days, and thus probably they had a native oxide layer close to 1 nm. XPS taken with a larger photon energy to have a mean free path of *ca*. 2 nm (Figure 3b or S12-top) permits to see the clean Ge layer underneath the native oxide, even for flakes exposed to air.

The formation of α-Ge NLs with well-defined orientations suggests that the wet ball-milling process induces cleavage of the germanium crystallites. Silicon, germanium, and diamond typically cleave in the (111) plane.[13] The formation of a flat, homogenous surface of a well-defined crystalline orientation (cleavage) *vs*. fracture is a complex process governed by several factors. On the one hand, silicon and germanium cleave only under tension, so that if a bending force is applied, cleavage is observed only in the area under tension (upper half of the new surface), while fracture appears in the lower half (under compression).[13] Additionally, the effects of the environment on the fracture behaviour of germanium have been well-known for a long time.[14] The cleavage behaviour of germanium in an etching solution is very different from the behaviour in air. The role of the solution might be both to induce local cracks and to reduce surface tension. The critical crack length is directly proportional to the surface energy and previous findings indicate that the surface energy in air is greater than in a solution.[15] Finally, the oxidation of a cleaved Ge surface is not expected, as GeO_2 is soluble in water (0.447 g in 100 mL water at 25 ℃)[16] and should not be present during the cleavage process. The cleavage of a thin macroscopic wafer of silicon or germanium is triggered by a shock wave applied normal to the crystallographic plane of minimum bond strength.[17] This is to some extent contrary to the usual technique of cleaving, consisting of applying force with a sharp knife in a direction parallel to the cleavage plane. In the case of silicon and germanium, the tendency to split smoothly is enhanced by a homogeneous stress concentration around the crystal, so that its crystallographic plane of minimum bond strength, which is the (111) plane, is intersected. Under these conditions, a shock wave will trigger the cleavage of a (111) wafer if it is directed normal to the cleavage plane. It is not preposterous to think that all or parts of these conditions are fulfilled in our case: reduction of surface tension, homogeneous radial stress and shock waves induced by the wet ball-milling process.

In order to identify the most likely surface terminations, we have computed, using density functional theory (DFT), the surface formation energy, considering low-Miller-index (100),

(110), and (111) surfaces and a high-Miller-index (211) surface. The surface energy is defined as the energy required to create a new surface and, thus, it can be determined by taking the energy difference between the total energy of a slab and an equivalent bulk reference amount of material. Using a super-cell model for each slab, the surface energy of a clean surface at T = 0 K, γ, can be obtained as,

$$\gamma = \frac{1}{2A}\left(E_{slab}^{total} - E_{bulk}^{ref}\right)$$

where E_{slab}^{total} and E_{bulk}^{ref} are the total energies of the slab and the bulk reference, respectively, A is the surface unit area, and the factor 1/2 is needed to account for the two surfaces of the slab. The results presented in Supplementary Table S2 manifest that the reconstructed (100) surface plane is the lowest in energy with a small advantage over the reconstructed (110), and unreconstructed (111) and (112). This is somewhat unexpected. Note, however, that we have taken into consideration surface reconstruction for some orientations. Still, we have not exhausted all possibilities since some can involve very large supercells, particularly in the (111) surface case. [11] A few of these reconstructions are shown in Figure S21. Also, we have not considered in this analysis adsorbates and contamination, which may stabilize unreconstructed surfaces, although their effect is taken into account when analysing the electronic properties of the slabs (Supporting Information section 10). Overall, these results are compatible with our experimental findings, as shown below.

Transmission electron microscopy (TEM), high-resolution TEM (HRTEM) and electron diffraction measurements carried out on isolated α-Ge NLs (**Figure 4**a-c and S3), confirm further the crystallinity of the material. We used aberration-corrected scanning transmission electron microscopy (STEM) combined with EELS techniques to investigate the local structure and chemistry of the nanolayers. Figure 4d presents atomic resolution high angle annular dark-field (HAADF) images of different α-Ge NLs showing three different crystal structures obtained with the electron beam down the [111] (left panel), [110] (most commonly found,

central panel) and [112] (right panel) directions (Figure 4d bottom panels show the structures corresponding to these projections), obtained at an acceleration voltage of 200 kV. We do not observe major defects, confirming the high crystalline quality of the samples.

The combination of imaging and EELS techniques has allowed us to determine the composition of the α-Ge NLs. Figure S15a exhibits two simultaneously acquired high-resolution ABF and HAADF images measured on the edge of a flake, in which a very thin amorphous layer, with an estimated thickness close to 1 nm, can be clearly observed in the ABF image. Some O and other impurities, such as minor amounts of Ca can also be detected within this layer. Additionally, Figure S15b shows a series of relative composition maps (in atomic percent) generated by analysing the Ca $L_{2,3}$, O K and Ge $L_{2,3}$ edges. Small amounts of Ca (in few units percent) are detected on the edges, along with some degree of oxidation. On the flakes, minor oxidation is detected, the total amount in the <5 atomic% range. This signal probably comes from the surface of the flakes, where a nm thick amorphous layer, such as the one observed at the edges, can be expected.

The crystal cleavage along different crystallographic planes generates dangling bonds that, as inferred from the XPS data shown in Figure 3b, are passivated with oxygen. More specifically, considering the high surface sensitivity at the used photon energies in XPS and the Raman data, these results suggest that the α-Ge NLs outmost layer presents mainly Ge-O bonds, formed upon breakage of the Ge-Ge bonds taking place during the crystal exfoliation and air exposure before the XPS analysis, while the formation of some Ge-H bonds cannot be discarded. Therefore, apart from potential crystal surface reconstruction to accommodate this new structure, germanium can saturate these sites forming new bonds (*e.g.* Ge-O or Ge-H bonds) with molecules present in the experimental conditions.

The exfoliation procedure leads to the production of α-Ge NLs with different thicknesses, small enough that the band gap may increase due to quantum confinement. In order to assess this

10

issue, we have again performed DFT calculations of their band structures, considering different situations for the main set of nanolayers identified by HRTEM: *i*) (111), (110) and (112) projected atomic structures, *ii*) different thicknesses, and *iii*) different surface germanium saturations or surface layer reconstructions (Supporting Information section 10). Notice that other higher Miller index orientations are usually conformed by the aggregation of small steps along lower indexes directions.

Figure 5a shows the calculated band gap for single- and four-layer α-Ge NLs with the above-mentioned orientations. The germanium surface atoms have been saturated with H atoms to suppress dangling bonds (similar results are obtained upon OH saturation, see Supporting Information section 10) following our experimental observations. It is worth mentioning that a direct band gap is obtained up to 6-7 monolayers, *i.e.*, α-Ge NLs of *ca*. 3 nm in thickness with an appreciable energy variation upon a diminution of nanolayer thickness down to 1 nm (Figure 5b). This variation is significant in the case of the (110) and (112) surfaces with the band gap increase up to 2.0 eV at 1 nm thickness and almost negligible in the (111) case. Note also that we are presenting results using a standard approximation (GGA) to our functional. It is well known that bulk germanium does not present a gap in this approximation, as it can be already anticipated in Figure 5b for the (111) surface where the gap is almost closed. Improved calculations using a hybrid functional (Supporting Information section 10) open a gap in the bulk structure and increase the gap of the slabs, but do not change the relative gap evolution with thickness in this range.

In order to experimentally confirm the band gap modulation with nanolayer thickness, we carried out structural and band gap measurements of α-Ge NLs by STEM-EELS using a monochromated Nion UltraSTEM 100MC HERMES working at 60 kV. This microscope allows spectral analysis with energy resolution around 15 meV.[18] We chose α-Ge NLs tilted,

so that the electron beam would be parallel to the [111] and [112] directions for the analysis. Figure 5c depicts the band gap of the sample as a function of the thickness for a flake oriented along the [112] direction. The band gap value on the edges of the sample is higher than that in the bulk, being about 0.85 eV on the edges and decreasing down to 0.65 eV on thicker α-Ge NLs. Figure 5d displays the lateral variations of the thickness of the [112] oriented α-Ge NLs, in layers down to a thickness of 2.5 nm (notice that measurements below this value show a large dispersion in band gap values as a consequence of the oxide layer). Similar measurements carried out in α-Ge NLs with [111] orientation do not show a band gap dependence with the thickness but rather a constant value (Figure S14). These experimental results agree with the theoretical band gap calculations in which only for very small thicknesses a band gap variation is expected for the [111] orientation, out of the experimental detection limit, while a larger variation is predicted for the [112] orientation (Fig. 5b). As already mentioned, flakes oriented so that the electron beam lies down the [112] direction probably present oriented surfaces or terraces in the <110> directions, since they are energetically more favourable. In any case their gap behaviour with thickness is rather similar and in qualitative agreement with the predictions.

In summary, we have shown that using a wet ball-milling procedure, we have successfully exfoliated bulk crystals of α-germanium yielding nanolayers with thicknesses down to *ca*. 2.5 nm, in which the crystallinity and structure is retained. The so-formed α-Ge NLs show a partial surface oxidation of *ca*. 1 nm acting as a passivation layer. Although, the germanium exfoliation is a complex process governed by several experimental factors, it is clear that implies the breakage of Ge-Ge covalent bonds along the most favourable energetic cleavage planes, as suggested by our theoretical calculations, where the solvent plays a key role preventing complete germanium oxidation.

The band gap in the nanolayers showing the (111) orientation does not change with thickness, remaining at a value near 0.45 eV, which is slightly lower than that expected for the bulk crystal.

Meanwhile, the nanolayers showing the (112) orientation present band gap up to 0.85 eV, values that depend on their thickness, which decrease around 0.15 eV when the specimen thickness increases just a few nanometers, to reach a constant value of *ca*. 0.6–0.7 eV, which is the one expected for bulk α-germanium. Noteworthy, theoretical calculations point to a further band gap increase up to 2.0 eV upon thickness decrease down to 1 nm. Based on these findings, we envision potential application of these new α-Ge NLs in (opto)electronics. Moreover, we propose to extend this procedure to other covalent crystals where exfoliation is considered not feasible. This would initiate a new family of 2D nanomaterials with original physicochemical properties.

Acknowledgements

References

[1]   a) S. Z. Butler, *et al*, ACS Nano 2013, 7, 2898; b) A. C. Ferrari, *et al*, Nanoscale 2015, 7, 4598; c) X. Ling, H. Wang, S. Huang, F. Xia, M. S. Dresselhaus, Proc. Nat. Ac. Sci. 2015, 112, 4523.

[2]   K. S. Novoselov, V. I. Fal'ko, L. Colombo, P. R. Gellert, M. G. Schwab, K. Kim, Nature 2012, 490, 192.

[3]   D. Akinwande, C. Huyghebaert, C. H. Wang, M. I. Serna, S. Goossens, L. J. Li, H. P. Wong, F. H. L. Koppens, Nature 2019, 573, 507.

[4]   A. Puthirath Balan, S. Radhakrishnan, C. F. Woellner, S. K. Sinha, L. Deng, C. d. L. Reyes, B. M. Rao, M. Paulose, R. Neupane, A. Apte, V. Kochat, R. Vajtai, A. R. Harutyunyan, C.-W. Chu, G. Costin, D. S. Galvao, A. A. Martí, P. A. van Aken, O. K. Varghese, C. S. Tiwary, A. Malie Madom Ramaswamy Iyer, P. M. Ajayan, Nat. Nano. 2018, 13, 602.

[5]   X. Xiao, X. Li, S. Zheng, J. Shao, H. Xue, H. Pang, Adv. Mat. Interf. 2017, 4, 1600798.

[6]   E. Bianco, S. Butler, S. Jiang, O. D. Restrepo, W. Windl, J. E. Goldberger, ACS Nano 2013, 7, 4414.

[7]   a) Z. Ni, Q. Liu, K. Tang, J. Zheng, J. Zhou, R. Qin, Z. Gao, D. Yu, J. Lu, Nano Letters 2012, 12, 113; b) M. E. Davila, G. Le Lay, Sci. Rep. 2016, 6, 20714.

[8]   D. Hanlon, *et al*, Nat. Comm. 2015, 6, 8563; K. R. Paton, E. Varrla, C. Backes, R. J. Smith, U. Khan, A. O'Neill, C. Boland, M. Lotya, O. M. Istrate, P. King, T. Higgins, S. Barwich, P. May, P. Puczkarski, I. Ahmed, M. Moebius, H. Pettersson, E. Long, J. Coelho, S. E. O'Brien, E. K. McGuire, B. M. Sanchez, G. S. Duesberg, N. McEvoy, T. J. Pennycook, C. Downing, A. Crossley, V. Nicolosi, J. N. Coleman, Nat. Mat. 2014, 13, 624.

[9]   P. Nemes-Incze, Z. Osváth, K. Kamarás, L. P. Biró, Carbon 2008, 46, 1435.

[10]   S. K. Sahari, H. Murakami, T. Fujioka, T. Bando, A. Ohta, K. Makihara, S. Higashi, S. Miyazaki, Jpn. J. Appl. Phys. 2011, 50, 04DA12.

[11]   Q. Chen, L. Liang, G. Potsi, P. Wan, J. Lu, T. Giousis, E. Thomou, D. Gournis, P. Rudolf, J. Ye, Nano Lett. 2019, 19, 1520.

[12]   J. Ouyang, C. Feng, X. Ji, L. Li, H. K. Gutti, N. Y. Kim, D. Artzi, A. Xie, N. Kong, Y.-N. Liu, G. J. Tearney, X. Sui, W. Tao, O. C. Farokhzad, Angew. Chem. Int. Ed. 2019, 58, 13405.

[13]   G. W. Gobeli, F. G. Allen, J. Phys. Chem. Sol. 1960, 14, 23.

[14]   T. L. Johnston, R. J. Stokes, C. H. Li, Acta Metal. 1958, 6, 713.

[15]   A. A. Griffith, G. I. Taylor, Philos. Trans. R. Soc. Lond., Ser. A 1921, 221, 163.

[16]   R. C. Weast, *CRC Handbook of Chemistry and Physics* Vol. 80-81, CRC Press, 1969.

[17]   F. Wilkes Donald, *US Patent US 4244348 A*, 1981.

[18]   O. L. Krivanek, T. C. Lovejoy, N. Dellby, T. Aoki, R. W. Carpenter, P. Rez, E. Soignard, J. Zhu, P. E. Batson, M. J. Lagos, R. F. Egerton, P. A. Crozier, Nature 2014, 514, 209.
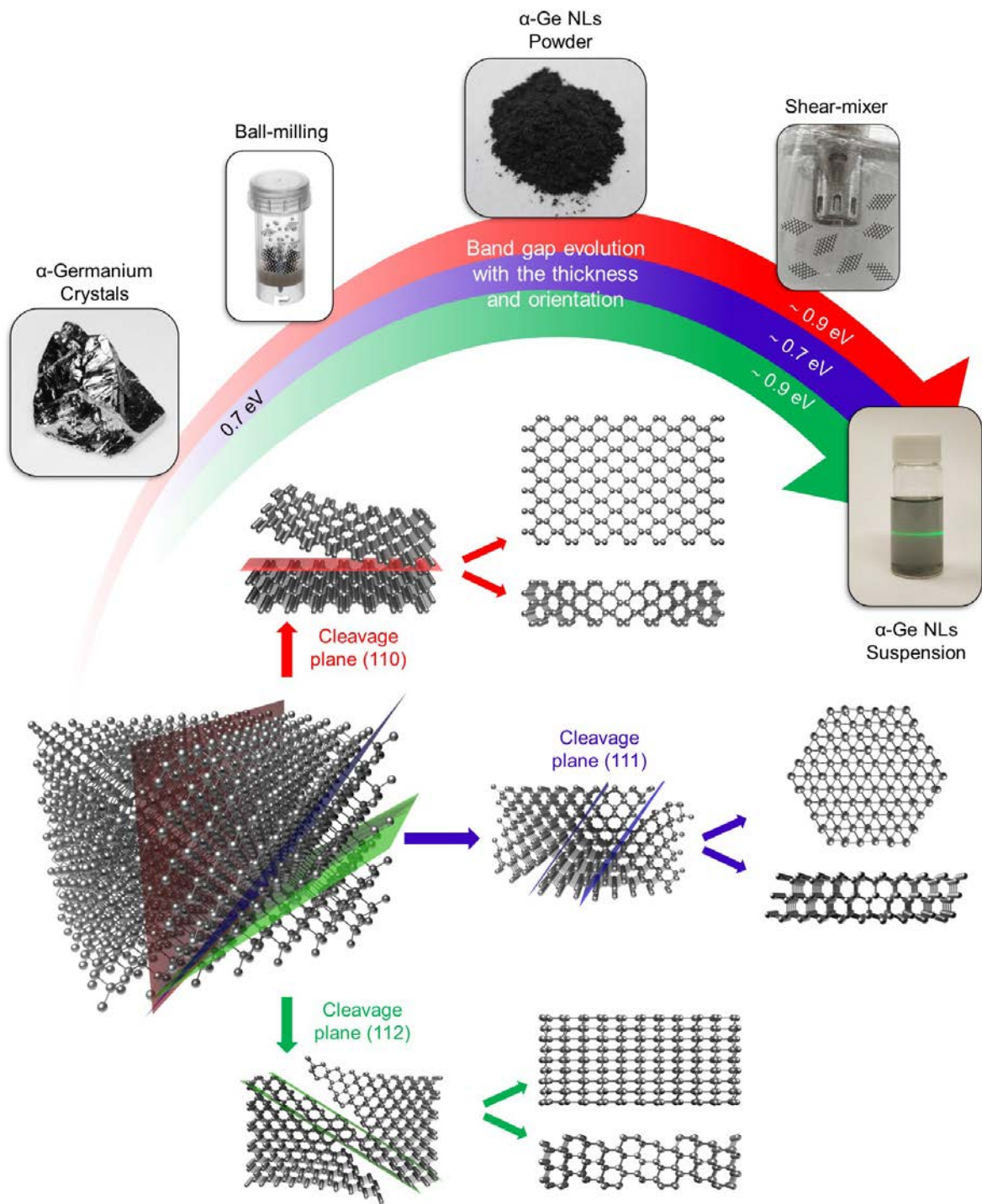
Figure 1. Schematic illustration of the preparation process to obtain α-Ge NLs powder and suspension and the band gap evolution with the thickness variation of the α-Ge NLs.
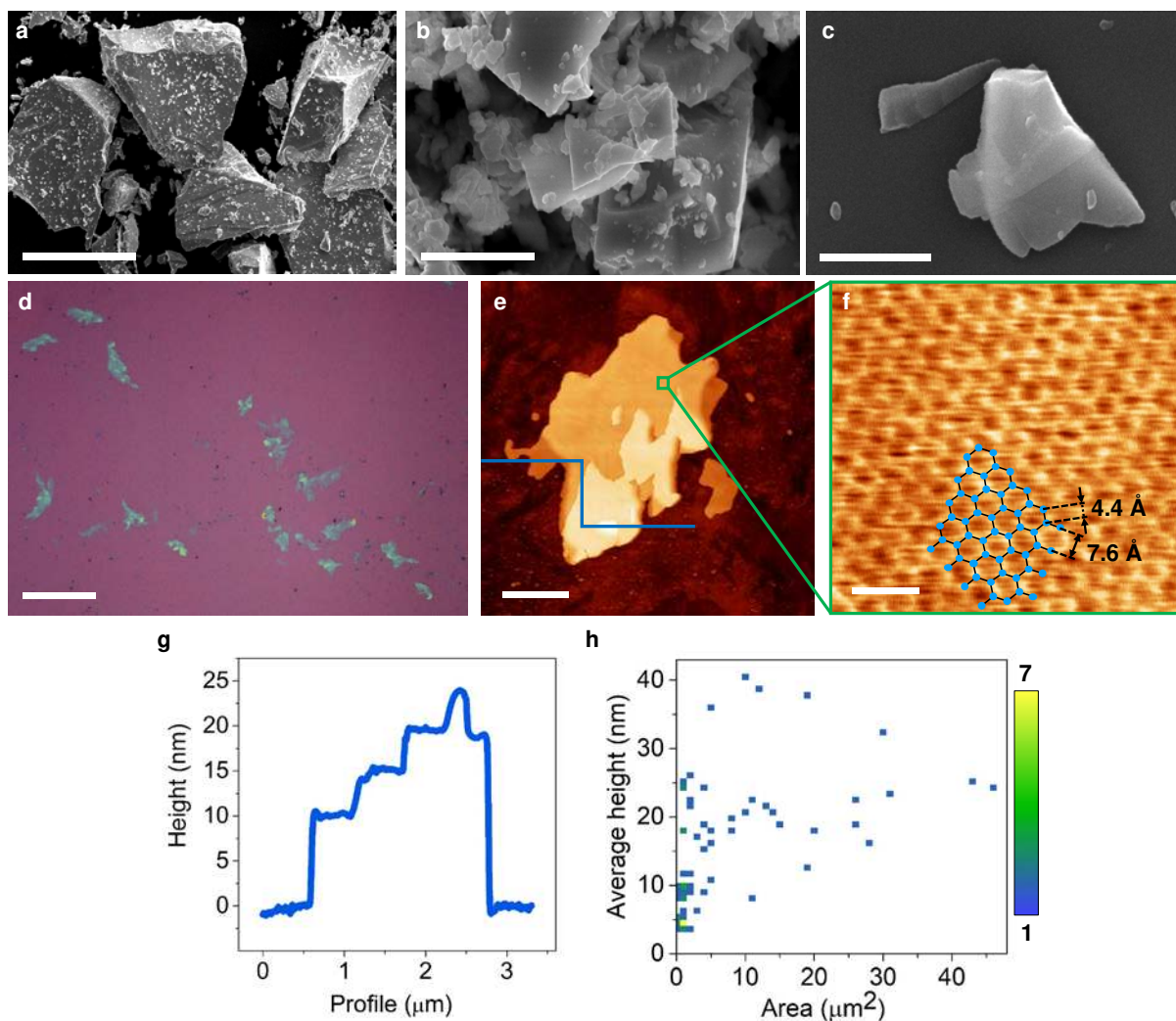
Figure 2. a) SEM image of bulk α-germanium crystals (scale bar: 50 μm), b) SEM image of α-Ge NLs powder (scale bar: 2 μm), c) SEM image of α-Ge NLs isolated from an α-Ge NLs suspension (scale bar: 500 nm), d) Optical image of α-Ge NLs isolated onto SiO_2 (scale bar: 20 μm), e) Topographic AFM image of an α-Ge NL on SiO_2 showing well-defined shapes, f) High resolution AFM image of an α-Ge NL deposited on SiO_2, taken on the marked region in (e) showing the hexagonal structure of the (111) orientation (scale bar: 2 nm), g) Height profile along the blue line in (e), h) 2D histogram plot of the number (color scale) of α-Ge NLs as a function of their height and area.
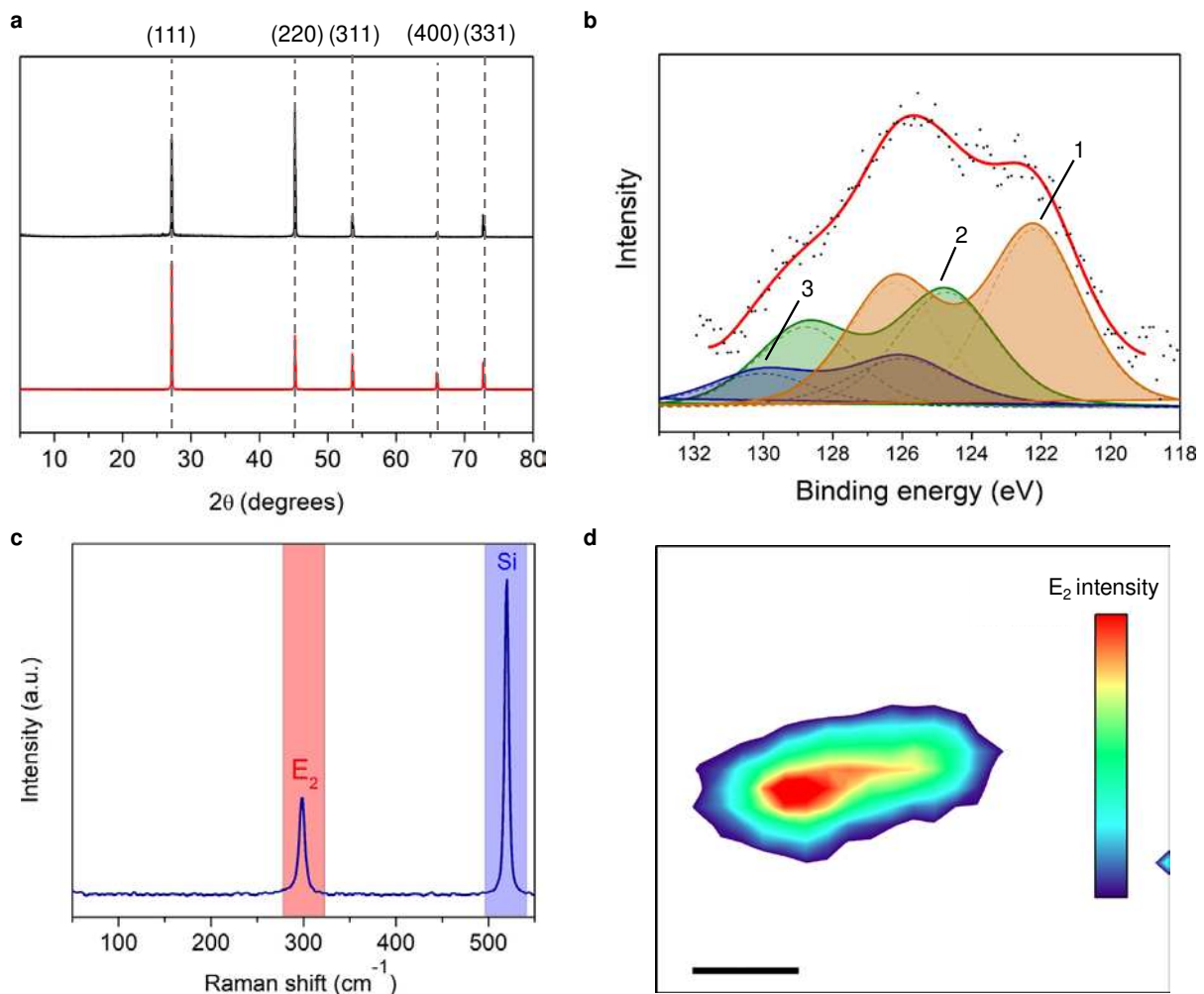
Figure 3. a) PXRD patterns of bulk α-germanium crystals (red) and α-Ge NLs (black), b) Typical XPS spectrum of Ge 3d peak (hν = 1253.6 eV) from α-Ge NLs. Numbers identify the different components: 1 (elemental Ge), 2 (Ge(II)) and 3 (Ge(IV)). Each component (full lines) corresponds to a Ge 3d doublet (dashed lines). Black dots are experimental points and the red line is the result of a fit, c) Single-point Raman spectrum of α-Ge NLs cast onto SiO_2 showing the peak of the E_2 vibrational mode of α-Ge NL as well as the silicon peak, d) Raman mapping of the E_2 vibrational mode intensity constructed by 625 single spectra using a green laser (λ_{exc} = 532 nm) and step-size of 0.2 μm (scale bar: 500 nm).
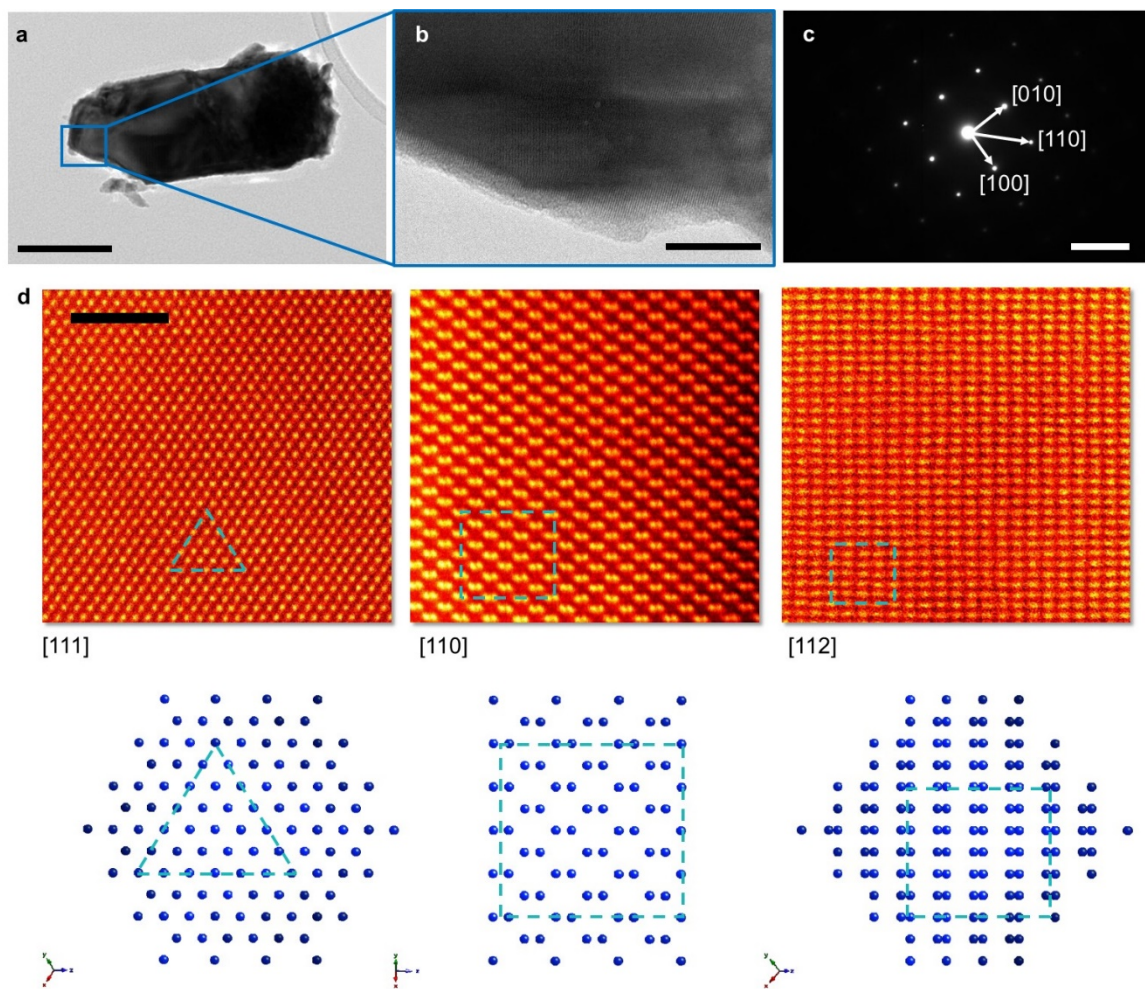
Figure 4. a) TEM image of an α-Ge NL isolated from an α-Ge NLs dispersion (scale bar: 200 nm), b) HRTEM of the blue area in (a) (scale bar: 10 nm), c) Electron diffraction pattern (scale bar: 5 nm^{-1}), d) Top panels: HAADF (high-angle annular dark field) images of sub-nanometric α-Ge NLs acquired using a 200 kV acceleration voltage in different zone axes, as indicated. Bottom panels: models of the crystallographic planes of the α-Ge structures shown in the top panels.
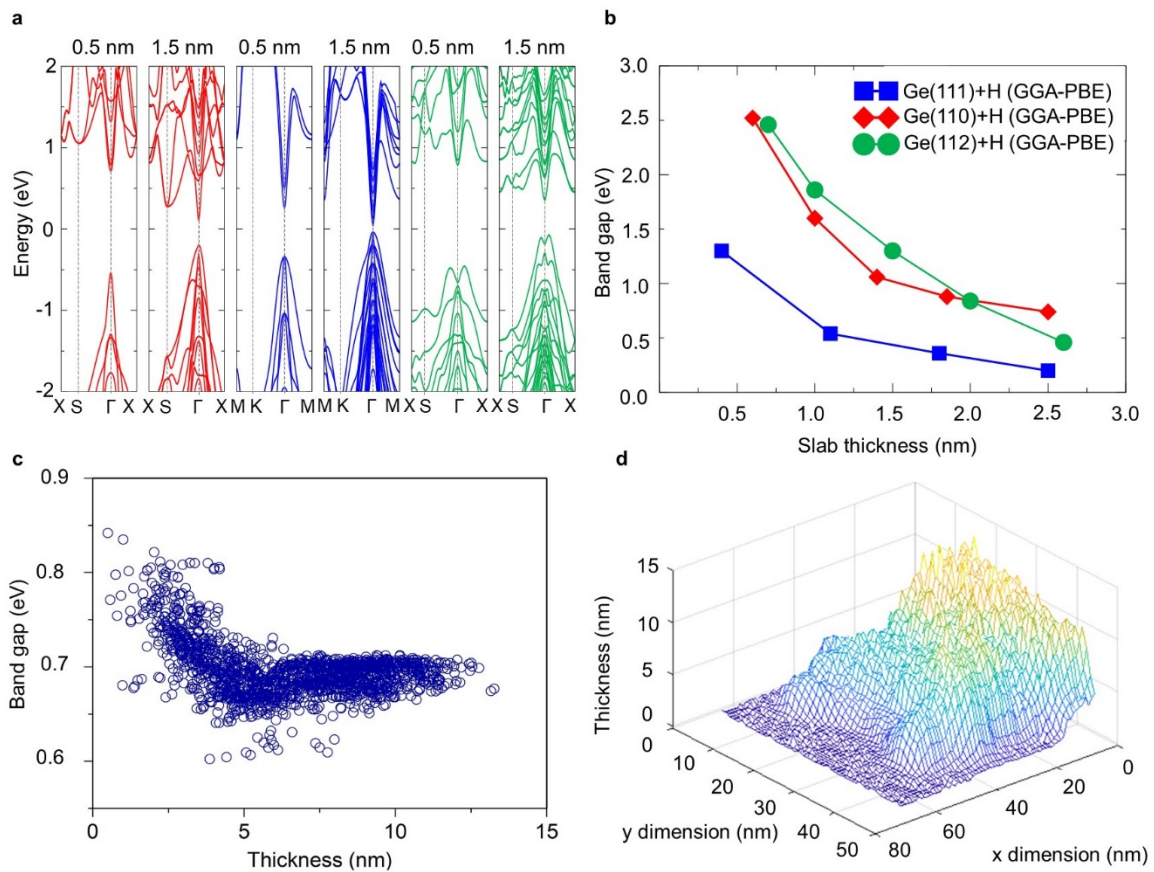
Figure 5. a) Calculated band structure of single- and four-layer α-Ge NLs with (110), red line, (111) blue line and (112), green line, orientations, b) Theoretical band gap value *versus* thickness for α-Ge NLs with (110), red line, (111), blue line, and (112), green line orientations, c) Measurements of the band gap variation with the thickness for α-Ge NLs obtained with the electron beam down the [112] direction using STEM combined with EELS, d) Mapping of a part of an α-Ge NL showing the variations of the sample thickness of the α-Ge NLs with [112] orientation.

The table of contents entry

α-Germanium crystals are exfoliated using a wet ball-milling technique to produce α-germanium nanolayers (α-Ge NLs) in a process that has been up-scaled to gram production. The α-Ge NLs can be redispersed using a shear-mixer, yielding very stable suspensions. Theoretical calculations predict a thickness-dependent bandgap of these nanolayers that has been confirmed by electron energy-loss spectroscopy (EELS) of α-Ge NLs with different orientations.

Keyword: alpha-germanium, exfoliation, band gap.

Carlos Gibaja,[1] David Rodríguez-San-Miguel,[1] Wendel S. Paz,[2,3] Iñigo Torres,[1] Elena Salagre,[2] Pilar Segovia,[2] Enrique G. Michel,[2] Mhamed Assebban,[4,5] Pablo Ares,[2,6] David Hernández-Maldonado,[7,8] Quentin Ramasse,[8,9] Gonzalo Abellán,[4,5] Julio Gómez-Herrero,[2,10] Maria Varela,[7] Juan José Palacios,[2,10] Félix Zamora[1,*]

Exfoliation of alpha-germanium: a covalent diamond-like structure